THE JOURNAL OF PHYSICAL CHEMISTRY B
A JOURNAL OF THE AMERICAN CHEMICAL SOCIETY

pubs.acs.org/JPCB
Article

Understanding the Mid-Infrared Spectra of Protic Ionic Liquids by Density Functional Theory

Yingzhen Chen, Christian Rodenbücher, Adrien Morice, Fabian Tipp, Piotr M. Kowalski, and Carsten Korte*

Cite This: J. Phys. Chem. B 2024, 128, 11723−11729
Read Online

ABSTRACT: Protic ionic liquids (PILs) are promising candidates as electrolytes for proton exchange polymer membrane fuel cells. In order to optimize their properties, a detailed understanding of the molecular interactions within the bulk and at the electrode−electrolyte interface is needed, which can be obtained by infrared spectra. A prerequisite for extracting information on the molecular structure and inter- or intramolecular interactions from an experimental spectrum is a reasonable interpretation of the observed spectral features. Here, we employed density functional theory to understand the vibration modes of PILs composed of ammonium cations and different counteranions. Different from the previous calculation methods performed on small cluster model systems consisting of isolated species, a periodically repeated system of four ion pairs was used in order to approximate the bulk liquid environment. The computed frequencies and IR intensity match well with the corresponding experimental spectra, allowing for its proper interpretation, especially the characteristic features of the interionic interaction. The presented approach enables accurate computation of a variety of ionic liquid systems in a highly efficient way.

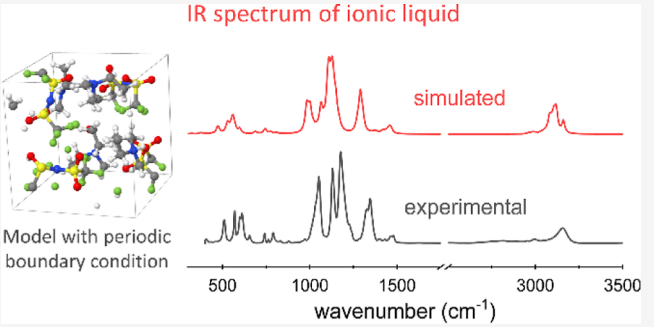

1. INTRODUCTION

Ionic liquids have attracted broad research interests due to their widespread applications, *e.g.*, as polar solvents in organic synthesis or as a lubricant with negligible vapor pressures.[1−3] Recently, an increasing number of studies are focusing on the use of ionic liquids as electrolytes for electrochemical energy conversion and storage,[4,5] due to their high electrochemical stability, high thermal stability, and nonflammability. Among different types of ionic liquids, protic ionic liquids (PILs), consisting of a cation with a Brønsted-acidic proton, have been considered as potential electrolytes for high-temperature proton exchange membrane fuel cells.[6−8] The properties and bulk structures of ionic liquids are complex due to varieties of intermolecular interactions such as Coulomb forces, hydrogen bonds, van der Waal forces, and steric repulsion. These interactions lead to the formation of ion pairs and nanoscaled domains due to ordering phenomena of cations and anions in the 10 nm range.[9] The related features can be revealed by means of spectroscopic techniques, such as infrared spectroscopy (IR).[10,11] However, the interpretation of the experimental vibrational spectra of ionic liquids is challenging. In this context, atomistic simulations based on density functional theory (DFT) have been employed on a regular basis to assist the interpretation of IR spectra.[11−13]

To assign the vibrational peaks observed in the experimental IR spectra of ionic liquids, DFT calculations on single isolated cation and anion species are often performed and the results are used as reference data.[10,14−17] This approach can identify some features of the measured spectrum resulting from the basic vibrational modes of the ion but could not contribute to simulating the spectral signatures arising from the interaction of anions and cations in a condensed phase. DFT calculations performed on ions pair have also been widely applied.[18−23] Although those improved the description of IR spectrum, the vibrational frequencies and IR intensities computed by this method often cannot reproduce the measured spectra sufficiently.[20] A more realistic approach to consider the interaction in a liquid phase consists of simulating the ionic species using a polarizable continuum model.[24] In such an approach, the ion pair (cluster) is placed in a void that is embedded in a dielectric environment with the experimental permittivity constant of the bulk liquid. The dielectric interaction of the ionic charges of the simulated ion pair with the other ions in the surrounding bulk is modeled as an averaged interaction with a continuous polarizable medium.[24]

Received: August 7, 2024
Revised: September 21, 2024
Accepted: September 23, 2024
Published: November 14, 2024

https://doi.org/10.1021/acs.jpcb.4c05084
J. Phys. Chem. B 2024, 128, 11723−11729

Owing to the lack of the exact value of the dielectric constants of the PILs, the dielectric constants of polar solvents (*e.g.*, dimethylformamide, ε_r = 37.22) and nonpolar solvents (*e.g.*, tetrahydrofuran, ε_r = 7.43) were applied in such calculations.[25] Applying an inaccurate dielectric constant may result in an incorrect prediction of the positions and number of absorption peaks. In particular, for PILs, the possible proton transfer in PILs leads to hydrogen bond networks. This is the case for PIL based on alkylammonium cations, in which strong hydrogen bonds exist between the active proton of the cation and the anion. The N−H stretching is sensitive to the environment and interionic interaction with the neighboring ions, resulting in various distinguishable local dielectric environments.

In order to overcome the limitations of the aforementioned methods, we applied an approach based on DFT simulations of a system consisting of four ion pairs with periodic boundary conditions so as to obtain a better approximation of a bulk-like liquid environment. A series of diethylmethylammonium $[Dema]^+$-based PILs with anions of different basicities and charge densities, *i.e.*, bis(trifluoromethanesulfonyl) imide $[TFSI]^-$ (bistriflimide), trifluoromethanesulfonate $[TfO]^-$ (triflate), hydrogen sulfate $[HSO_4]^-$, and methanesulfonate $[MsO]^-$ (mesylate), have been studied. This enabled a quantitative analysis of the mid-IR spectra as well as of the interionic interactions.

2. METHODS

2.1. Computational Methods. The IR spectra of four ionic liquids with the same cation but different counteranions were simulated with density functional perturbation theory (DFPT) using the Quantum ESPRESSO code with a plane-wave basis set.[26] The Perdew−Burke−Ernzerhof (PBE) exchange−correlation functional was applied.[27] The plane−wave cutoff energy was set to 30 Ry and the core electrons were replaced with ultrasoft pseudopotentials.[28] To model four ion pairs, the initial configurations were obtained by performing classical molecular dynamics (MD) simulation using the LAMMPS software package.[29] A unit cell with periodic boundaries in an isothermal−isobaric (*NPT*) ensemble was used for the preliminary relaxation. The temperature was set to be 298.15 K and the initial edge size of the cubic simulation box was 10 Å. The interactions between the ionic liquid molecules were modeled with the Optimized Potential for Liquid Simulations-All Atom (OPLS-AA) force field,[30−35] and the parameters are listed in the Supporting Information. An equilibration run was performed in 300,000 steps with 1 fs time steps in *NPT* conditions, using a Nosé−Hoover thermostat. As depicted in Table 1, the calculated densities of PILs after equilibration were in good agreement with experimental data found in the literature (within 6%),[36−38] which reflects the reliability of the applied force field.

Table 1. Comparison of Calculated Densities of PILs with the Experimental Ones[a]

PIL	$\rho_{20\ °C}$, literature (g cm^{-3})	ρ_{MD}, this work
[Dema][TfO]	1.291[36]	1.344 g cm^{-3} (+4.1%)
[Dema][MsO]	1.135[36]	1.116 g cm^{-3} (−1.7%)
[Dema][HSO_4]	1.235[37]	1.304 g cm^{-3} (−5.6%)
[Dema][TFSI]	1.453[37]	1.507 g cm^{-3} (+3.7%)

[a]Adapted from reference.[36,37] Copyright [2014] [2016], American Chemical Society.

The obtained atomic configurations were taken as input structures for the DFT simulations and a structural relaxation has been performed using the Quantum ESPRESSO code.[26] The calculations were performed by using the same periodic boundary conditions as those for the classical MD simulations. The relaxation of the atomic positions converged to a value for the residual forces of 1×10^{-4} Ry Bohr^{-1} for each atom. The vibrational analysis was performed on the DFT-optimized structures (see Figure S1) using DFPT as implemented in the PHonon tool of Quantum ESPRESSO package. In order to compare with the experimental spectra, the calculated, discrete IR spectra (based on a finite set of vibrational frequencies) were convoluted with the Lorentz profile curves with 20 cm^{-1} full width at half-maximum (fwhm). As a reference for comparing the results, the spectra of an isolated single PIL cation and anion as well as a single ion pair were also calculated, respectively. In order to prevent any interaction between the neighboring images, the isolated molecular species were computed in a cubic supercell with a cell length of 40 Å.

2.2. Infrared Spectroscopy Measurement. An FTIR spectrometer (Thermo Fisher Scientific, USA) with an attenuated total reflection unit (Monolithic diamond Gladi-ATR, PIKE technologies, USA) was employed to record the IR spectra of ionic liquids. The spectra were collected in the range between 400 and 4000 cm^{-1} with a spectral resolution of 4 cm^{-1}. A total of 32 scans were averaged per spectrum.

3. RESULTS AND DISCUSSION

Figure 1 illustrates the lowest-energy geometries of the $[Dema]^+$ cation and of the different anions, *i.e.*, $[TFSI]^-$, $[TfO]^-$, $[HSO_4]^-$, and $[MsO]^-$. The calculated IR spectra of the isolated cations and anions are plotted in Figure 2 as yellow curves and green curves, respectively. It is clear that the ν(NH) stretching vibration of an isolated single $[Dema]^+$ cation is located at 3291 cm^{-1}. The asymmetric and symmetric stretching vibrations of the C−H bonds of the methyl and ethyl groups, *i.e.*, the combined modes of $\nu_{as}(CH_3)$, $\nu_s(CH_3)$, $\nu_{as}(CH_2)$, and $\nu_s(CH_2)$, overlap in the range of 2900−3100 cm^{-1}.[1] The overlapping results in broad bands centered at 3055 and 2990 cm^{-1}. In the low wavenumber region, the peak at 1361 cm^{-1} is caused by the δ(N−H) bending mode, whereas the broad band at 1445 cm^{-1} is contributed by various bending modes of C−H, *i.e.*, combined modes of $\delta(CH_3)$, $\tau(CH_3)$, and $\omega(CH_3)$ from the methyl group and $\delta(CH_2)$, $\tau(CH_2)$, and $\omega(CH_2)$ from the ethyl groups. The bands at 965 and 822 cm^{-1} are primarily attributed to the combined ν_{as}(C−N−C) asymmetric stretching mode and ν(C−C) stretching modes.

As shown in the calculated spectrum of an isolated $[TFSI]^-$ anion, three intense peaks are found in the region of 800−1400 cm^{-1}. The absorption peak at 1309 cm^{-1} corresponds to the $\delta_{as}(SO_2)$ asymmetric stretching mode. The broad peak at 1129 cm^{-1}, accompanied by a shoulder at 1101 cm^{-1}, results from an overlap of various C−F and S−O stretching modes, *e.g.*, $\nu_s(CF_3)$, $\nu_{as}(CF_3)$, and $\nu_s(SO_2)$. The peak at 983 cm^{-1} corresponds to the ν_{as}(S−N−S) asymmetric stretching mode. A medium peak is also found at 581 cm^{-1}, which can be assigned to the ν_s(S−N−S) symmetric stretching mode and $\delta(SO_2)$ bending. The correspondence of the outlined spectral features calculated for the isolated ions to the experimental spectra is not obvious.

The simulated spectrum of isolated single pair of PIL is shown as a blue curve in Figure 2. The anion-type-dependent

https://doi.org/10.1021/acs.jpcb.4c05084
J. Phys. Chem. B 2024, 128, 11723−11729

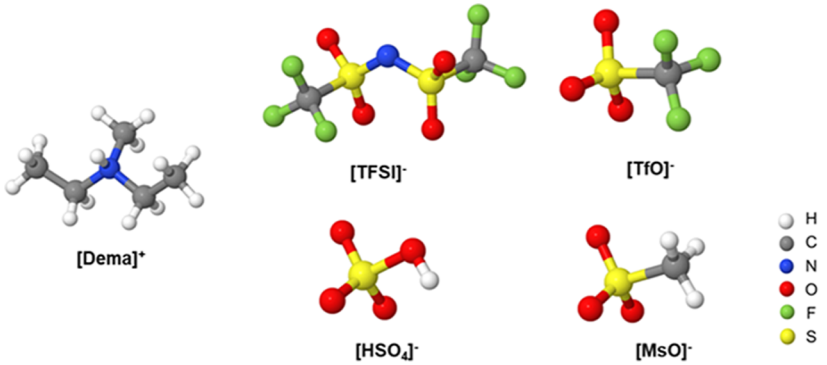

Figure 1. DFT-optimized structures of the $[Dema]^+$ cation and $[TFSI]^-$, $[TfO]^-$, $[HSO_4]^-$, and $[MsO]^-$ anion.

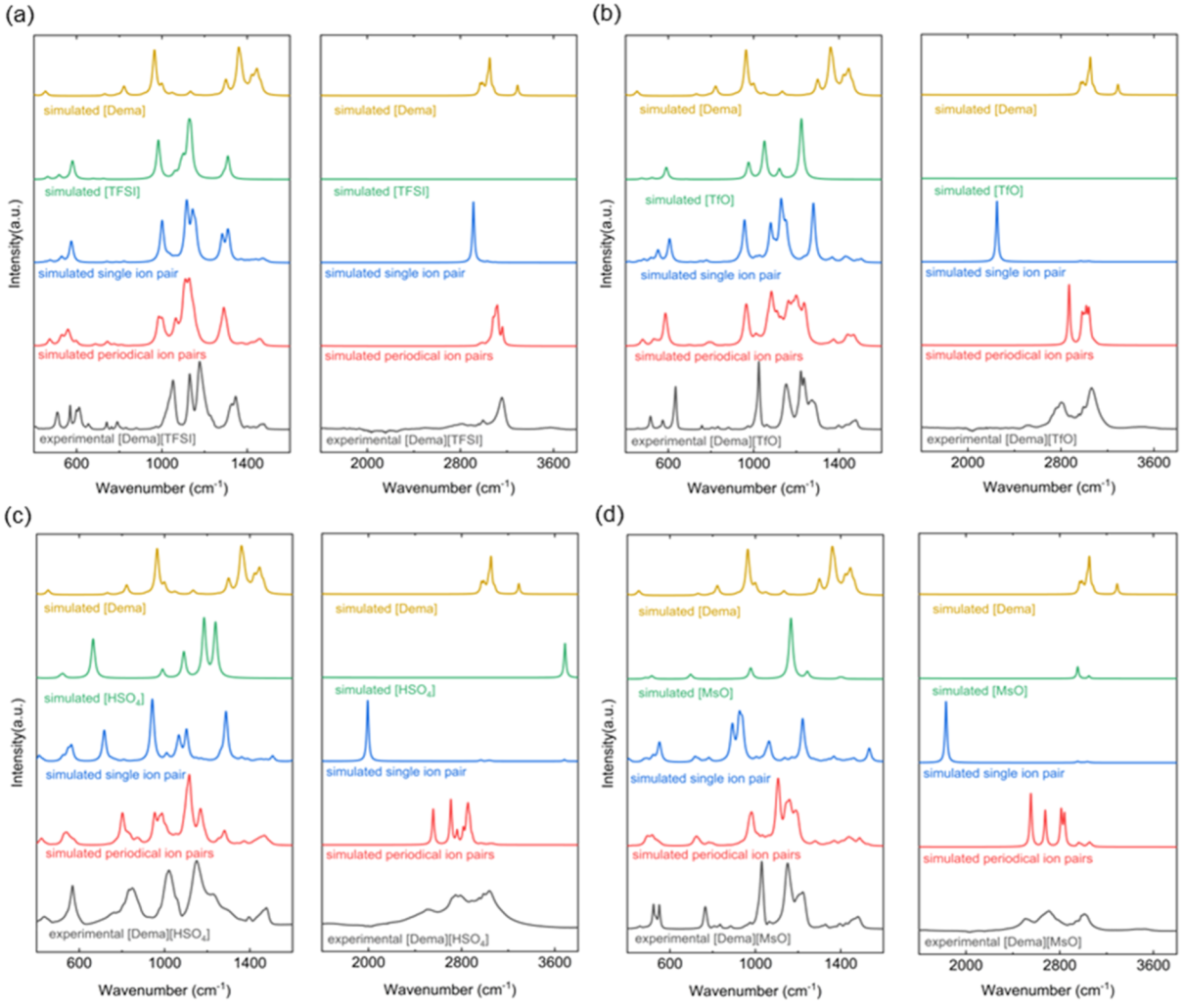

Figure 2. Simulated IR spectra of the PILs: (a) [Dema][TFSI], (b) [Dema][TfO], (c) $[Dema][HSO_4]$, and (d) [Dema][MsO]; yellow curve: simulation of one cation; green curve: simulation of one anion; blue curve: simulation of one single ion pair; red curve: simulation of four ion pairs with periodical boundary conditions; and black curve: experimental spectra.

shifts of the $[Dema]^+$ cation can be observed. The peak positions of these bands decrease in the order with [Dema][TFSI] > [Dema][TfO] > $[Dema][HSO_4]$ > [Dema]-[MsO], which correlates with increasing basicity of their counteranions. The frequency shifts can be related to different interaction strengths caused by different anions, which was also seen in previous studies of far-IR spectra of similar compounds.[41−47] Although simulations of single ion pairs lead to an improvement over results obtained with the isolated ions, the computed peak positions do not match well the position of the broad peaks between 2000 and 3600 cm^{-1} observed in the experimental spectra.

The spectra computed for periodical repeated systems of four ion pairs to approximate a bulk environment are plotted as red curves in Figure 2. In the calculated spectrum of [Dema][TFSI], intense bands can be observed at 1290,

https://doi.org/10.1021/acs.jpcb.4c05084
J. Phys. Chem. B 2024, 128, 11723−11729

Table 2. Wavenumber of the IR Band Observed in the Experimental Spectra Compared to the DFT-Calculated Wavenumber Calculation with the Periodic Boundary Condition[a]

Exp. wavenumber (cm^{-1})		Cal. wavenumber (cm^{-1})	vibration modes of [Dema][TFSI]	Exp. wavenumber (cm^{-1})		Cal. wavenumber (cm^{-1})	vibration modes of [Dema][TfO]
3157	m	3117	ν(NH)	3062	s	3039	ν(NH)
2993	w	2983	ν(CH)	2994	m	2983	ν(CH)
1479	w	1345	δ(NH)	2801	s	2862	ν(NH)
1346	s	1290	$\nu_{as}(SO_2)$	1479	m	1469	δ(NH)
1177	s	1123	$\nu_{as}(CF_3)$, $\nu_{as}(SO_2)$	1274	m	1236	$\nu_{as}(SO_3)$
1131	s	1066	$\nu_{as}(CF_3)$	1221	s	1164	$\nu_{s}(CF_3)$
1052	s	999	ν_{as}(SNS)	1153	s	1083	$\nu_{as}(CF_3)$
791	w	747	δ(CH), ν(CNC)	1024	s	966	$\nu_{s}(SO_3)$
741	w	688	ν_{s}(SNS)	757	w	788	δ(CH), ν(CNC)
612	m	559	$\delta_{ip}(SO_2)$	634	s	587	ν(CS)
570	m	531	$\delta_{op}(SO_2)$	574	m	534	$\delta(SO_3)$
510	m	474	$\delta(CF_3)$	516	m	481	$\delta(CF_3)$
Exp. wavenumber (cm^{-1})		Cal. wavenumber (cm^{-1})	vibration modes of [Dema][HSO_4]	Exp. wavenumber (cm^{-1})		Cal. wavenumber (cm^{-1})	vibration modes of [Dema][MsO]
3036	s	2855	ν(OH), ν(CH)	3005	s	2962	ν(CH)
2987	m	2760	ν(NH)	2708	s	2676	ν(NH)
2745	s	2707	ν(NH)	2507	s	2553	ν(NH)
2501	m	2555	ν(OH)	1479	s	1488	δ(NH)
1477	m	1468	δ(NH)	1210	m	1189	ν_{as}(CNC), δ(CH)
1225	m	1169	ν_{as}(CNC), δ(CH)	1151	s	1107	$\nu_{as}(SO_3)$
1150	s	1116	$\nu_{as}(SO_3)$	1030	s	982	$\nu_{s}(SO_3)$
1021	s	988	$\nu_{s}(SO_3)$	765	m	724	ν(CS)
849	s	802	δ(SOH)	550	s	517	$\omega(SO_3)$
568	s	540	$\delta(SO_3)$	523	s	495	$\tau(SO_3)$

[a]The symbol s, m, and w indicate the strong, medium, and weak peak observed in the spectra, respectively, and the notation ν_s, ν_{as}, δ_{ip}, δ_{op}, ω, and τ represent the symmetric stretching, asymmetric stretching, in-plane bending, out−of plane bending, wagging, and twisting modes, respectively.

1123, 999, and 559 cm^{-1}, see Figure 2a. The shapes of these bands are similar, and their peak positions are almost the same with a shift of less than 25 cm^{-1}, as found for the calculated spectrum of a single isolated $[TFSI]^-$ anion. This indicates that the fingerprint signals in the spectral region of 800−1400 cm^{-1} are primarily contributed by the $[TFSI]^-$ anions. The ν(N−H) stretching mode from the cation can be found in the region of 3000−3200 cm^{-1}, overlapping with the C−H stretching modes. Thus, there is a red shift of about 200 cm^{-1} compared to the frequency of the ν(N−H) stretching mode of a single isolated $[Dema]^+$ cation. On the other hand, good match of the frequencies computed with the quasiharmonic approximation to the observed frequencies indicates suppression of anharmonic effects in a condensed phase. The δ(N−H) bending mode is blue-shifted and shows up at 1345 cm^{-1}. The superposition of ν_{as}(C−N−C) asymmetric stretching modes and ν(C−H) stretching modes results in the appearance of one broad but weak absorption peak centered at 747 cm^{-1}. The calculated spectrum, based on four ion pairs and periodic boundary conditions, agrees better with the important features of the experimental spectrum than when a comparison is made with the spectra calculated for isolated ions and ion pairs. The details of the comparison of the experimental spectrum and the calculated one are presented in Table 2.

The IR band profiles calculated for the other [Dema]-based ionic liquids, [Dema][TfO], [Dema][HSO_4], and [Dema][MsO], also match well the experimental spectra, especially in the wavenumber range of 400−1600 cm^{-1}, see Figure 2b−d. The assignments of the peaks are also listed in Table 2. The intense peaks observed at 1274, 1221, 1153, 1024, and 634 cm^{-1} in the experimental spectrum of [Dema][TfO] can be assigned to vibration modes of $[TfO]^-$, *i.e.*, the asymmetric stretching $\nu_{as}(SO_3)$, symmetric stretching $\nu_s(CF_3)$, asymmetric stretching $\nu_{as}(CF_3)$, symmetric stretching $\nu_s(SO_3)$, and wagging mode $\omega(SO_3)$, respectively. In the experimental spectrum of [Dema][HSO_4], the intense peaks at 1150, 1021, 849, and 568 cm^{-1} can be assigned to the asymmetric stretching $\nu_{as}(SO_3)$, the symmetric stretching $\nu_s(SO_3)$, and the bending mode δ(SOH). In the spectrum of [Dema][MsO], the intense peaks at 1151 and 1030 cm^{-1} can be assigned to the asymmetric stretching $\nu_{as}(SO_3)$ and symmetric stretching $\nu_s(SO_3)$, whereas the peak at 765 cm^{-1} corresponds to stretching ν(CS). This indicates again that the strong bands in the low wavenumber region are primarily contributed by the vibration modes from the corresponding anion of the ionic liquid.

According to the calculations, the C−N−C stretching and C−H bending modes of the cation can be found in the low-frequency region. The intensity is lower compared to the peaks assigned to the anions and are only visible as weak peaks in the range of 700−800 cm^{-1} in the spectra of [Dema][TFSI] and [Dema][TfO]; in other wavenumber ranges, these peaks are hidden due to an overlap with the peaks of the anion vibration modes. On the other hand, the C−H stretching modes can be found in the high wavenumber region. However, they have a lower intensity with respect to the N−H stretching modes and partially overlap with these. For example, in the experimental spectra of [Dema][TfO], the peaks related to the C−H stretching modes are found at 2994 and 2954 cm^{-1} and are superposed by a broad peak from the stretching mode of N−

https://doi.org/10.1021/acs.jpcb.4c05084
J. Phys. Chem. B 2024, 128, 11723−11729

H. The assignment of these C−H stretching modes is in agreement with experimental studies performed on a deuterium substitution. In the IR spectrum of deuterated [Dema][TfO], *i.e.*, with a $(C_2H_5)_2CH_3N\text{-}D^+$ cation, the relatively weak signals of the C−H stretching mode can be clearly observed, as the N-D signal is shifted to lower wavenumbers compared to N−H.[40]

The N−H bending mode of the $[Dema]^+$ cation gives rise to a medium peak at about 1480 cm^{-1} for the investigated PILs. The frequency of the N−H stretching modes varies for different ion pairs, *i.e.*, for different anions. As shown by the DFT simulations based on four ion pairs, each cation has a different frequency for the N−H stretching mode, giving rise to four different peaks in the spectrum. The N−H stretching modes can be found at 3161, 3124, 3118, and 3106 cm^{-1} in the case of [Dema][TFSI], whereas in the case of [Dema][TfO], these peaks are shifted to lower frequencies, 3038, 3017, 3000, and 2981 cm^{-1}. For [Dema][HSO_4] and [Dema][MsO], they appear at 2891, 2855, 2844, and 2814 cm^{-1} and at 2840, 2813, 2676, and 2553 cm^{-1}, respectively. In comparison with the experimental spectra, broad bands in the corresponding regions are measured. In the experimental spectrum of [Dema][TFSI], a broad band exists centered at 3157 cm^{-1}. Two broad bands at 3062 and 2801 cm^{-1} were observed for [Dema][TfO], but at 3036 and 2745 cm^{-1} for [Dema][HSO_4] and at 3005 and 2708 cm^{-1} for [Dema][MsO]. The computed peak positions match well the experimentally measured features, which indicates that variable structural arrangements in the direct vicinity of the cations of the ionic liquid are an origin of the variability of the high-frequency, H−N vibrational mode.

Overall, the simulated results based on a model with four ion pairs in a periodic box describe well the experimental vibrational spectra of all investigated PILs and represent a significant improvement compared with the calculations based on isolated ions or a single ion pair. This modeling approach is able to approximate the environment of the ions in the bulk of an ionic liquid and reveals their characteristic features due to the interionic interaction between the cations and anions. All of the ionic liquids considered are composed of a $[Dema]^+$ cation. The results indicate that the N−H bond in the $[Dema]^+$ cation is highly influenced by the presence of the counteranion and its structure. The shift of the ν(N−H) stretching mode is found in the experimental and calculated IR spectra. In the case of an isolated $[Dema]^+$ cation, the N−H stretching mode is located at 3290 cm^{-1}. The presence of an anion in close proximity leads to the formation of a hydrogen bond with the oxygen atoms N−H···O of the anion. The presence of the H-bond is shown by X-ray diffraction and NMR spectroscopy. The effect of H-bond on intermolecular interaction was also observed by Fumino et al. in the range from 100 to 300 cm^{-1} in the far-IR spectra of PILs based on $[(CH_3)_3NH]^+$ cation.[45−47] The formation of a hydrogen bond induces a general weakening of the N−H bond strength accompanied by an increase in the N−H bond length. Accordingly, the N−H stretching shifts to a lower frequency, *i.e.*, it is red-shifted. Regarding the extent of the observed red shift, there is a clear dependence on the basicity of the counteranion. A higher basicity of the anion decreases the charge density of the cation and strengthens the hydrogen bond. The broad N−H bands observed in the high-frequency region are explained by a superposition of slightly different N−H vibration modes in local perturbed environments due to thermal fluctuations in the real liquid. This is because the simulation using four ion pairs and periodic boundary conditions yields peak positions of the N−H stretching signals that correspond well with the position of the broad band observed in the experimental spectrum. Obviously, the model system consisting of four ion pairs has its limitations and cannot cover the entire range of N−H vibration modes realized in the real bulk environment of an ionic liquid, and for this reason, we cannot expect a perfect reproduction of observed high frequency, N−H mode feature.

4. CONCLUSIONS

We employed DFT with a periodically repeated system of four ion pairs to determine the vibration modes of bulk PILs. The simulated frequencies and intensities match well with the experimental spectra and represent a significant improvement when compared with simulations based only on isolated ions or small isolated clusters. The results indicate that the intense peaks in the low frequency region (below 1400 cm^{-1}) are mainly contributed by the vibration modes of the corresponding anion. There are only weak IR peaks due to the vibrational modes of the cation. The medium peak found at around 1480 cm^{-1} in all investigated ionic liquids can be assigned to the N−H bending mode. The N−H stretching frequencies give rise to peaks in the spectral range of 2500−3500 cm^{-1}. The shift in the N−H stretching in the ammonium-based ionic liquids was found to be dependent on the strength of the interaction between the cation and anion by hydrogen bonds. The formation of hydrogen bonds with the anion induces a weakening of the N−H strength and so leads to a shift toward a lower wavenumber in the spectra. The calculations reveal that the thermal fluctuations in the local environment of the hydrogen bond lead to a distribution of slightly modified bond strengths and, thus, to a broad IR band. This study demonstrates that it is possible to accurately simulate the structural features of a bulk ionic liquid and its IR spectral response with a model system of a few ions in a periodically repeated simulation box.

■ ASSOCIATED CONTENT

Supporting Information

The Supporting Information is available free of charge at https://pubs.acs.org/doi/10.1021/acs.jpcb.4c05084.

Force field parameters for MD simulation and DFT-optimized structure of ionic liquids (PDF)

■ AUTHOR INFORMATION

Corresponding Author

Carsten Korte − *Institute of Energy Technologies—Electrochemical Process Engineering (IET-4), Forschungszentrum Jülich GmbH, Jülich 52425, Germany; RWTH Aachen University, Aachen 52062, Germany;* orcid.org/0000-0001-6574-6223; Email: c.korte@fz-juelich.de

Authors

Yingzhen Chen − *Institute of Energy Technologies—Electrochemical Process Engineering (IET-4), Forschungszentrum Jülich GmbH, Jülich 52425, Germany; RWTH Aachen University, Aachen 52062, Germany;* orcid.org/0000-0002-0809-5521

Christian Rodenbücher − *Institute of Energy Technologies—Electrochemical Process Engineering (IET-4), Forschungszentrum Jülich GmbH, Jülich 52425, Germany;* orcid.org/0000-0001-8029-3066

Adrien Morice − *Institute of Energy Technologies—Electrochemical Process Engineering (IET-4), Forschungszentrum Jülich GmbH, Jülich 52425, Germany*

Fabian Tipp − *Institute of Energy Technologies—Theory and Computation of Energy Materials (IET-3), Forschungszentrum Jülich GmbH, Jülich 52425, Germany; Jülich Aachen Research Alliance, JARA Energy & Center for Simulation and Data Science (CSD), Jülich 52425, Germany;* orcid.org/0009-0009-6120-5660

Piotr M. Kowalski − *Institute of Energy Technologies—Theory and Computation of Energy Materials (IET-3), Forschungszentrum Jülich GmbH, Jülich 52425, Germany; Jülich Aachen Research Alliance, JARA Energy & Center for Simulation and Data Science (CSD), Jülich 52425, Germany;* orcid.org/0000-0001-6604-3458

Complete contact information is available at: https://pubs.acs.org/10.1021/acs.jpcb.4c05084

Author Contributions

Yingzhen Chen: Conceptualization, methodology, investigation, visualization, and writing—original draft, review, and editing; Christian Rodenbücher: methodology, project administration, and writing—review and editing; Adrien Morice: investigation and writing—review and editing; Fabian Tipp: investigation; Piotr Kowalski: methodology, resource, and writing—review and editing; Carsten Korte: supervision, funding acquisition, project administration, and writing—review and editing.

Notes

The authors declare no competing financial interest.

■ ACKNOWLEDGMENTS

Y. Chen acknowledges the financial support of the Federal Ministry for Economic Affairs and Energy of Germany (HiFi-PEFC Project No. 03ETB003A). We also acknowledge the JARA−CSD partition of supercomputing resources granted through project cjiek61. We gratefully acknowledge C. Wood for proofreading the manuscript.

■ ADDITIONAL NOTE

[1]Symbols used to specify a vibration mode: symmetric stretching (ν_s), asymmetric stretching (ν_{as}), symmetric bending (δ_s), asymmetric bending (δ_{as}), wagging (ω), and twisting (τ).[39]

■ REFERENCES

(1) Wasserscheid, P.; Welton, T. *Ionic Liquids in Synthesis*; Wiley, 2007.

(2) Zhou, Y.; Qu, J. Ionic Liquids as Lubricant Additives: A Review. *ACS Appl. Mater. Interfaces* **2017**, *9*, 3209−3222.

(3) Amarasekara, A. S. Acidic Ionic Liquids. *Chem. Rev.* **2016**, *116*, 6133−6183.

(4) Armand, M.; Endres, F.; MacFarlane, D. R.; Ohno, H.; Scrosati, B. Ionic-liquid materials for the electrochemical challenges of the future. *Nat. Mater.* **2009**, *8*, 621−629.

(5) Wang, X.; Salari, M.; Jiang, D.; Chapman Varela, J.; Anasori, B.; Wesolowski, D. J.; Dai, S.; Grinstaff, M. W.; Gogotsi, Y. Electrode material−ionic liquid coupling for electrochemical energy storage. *Nat. Rev. Mater.* **2020**, *5*, 787−808.

(6) Nakamoto, H.; Watanabe, M. Brønsted acid-base ionic liquids for fuel cell electrolytes. *Chem. Commun.* **2007**, 2539−2541.

(7) Lee, S.-Y.; Ogawa, A.; Kanno, M.; Nakamoto, H.; Yasuda, T.; Watanabe, M. Nonhumidified intermediate temperature fuel cells using protic ionic liquids. *J. Am. Chem. Soc.* **2010**, *132*, 9764−9773.

(8) Wippermann, K.; Korte, C. Effects of protic ionic liquids on the oxygen reduction reaction—a key issue in the development of intermediate-temperature polymer-electrolyte fuel cells. *Curr. Opin. Electrochem.* **2022**, *32*, 100894.

(9) Hayes, R.; Warr, G. G.; Atkin, R. Structure and nanostructure in ionic liquids. *Chem. Rev.* **2015**, *115*, 6357−6426.

(10) Moschovi, A. M.; Ntais, S.; Dracopoulos, V.; Nikolakis, V. Vibrational spectroscopic study of the protic ionic liquid 1-H-3-methylimidazolium bis(trifluoromethanesulfonyl)imide. *Vib. Spectrosc.* **2012**, *63*, 350−359.

(11) Paschoal, V. H.; Faria, L. F. O.; Ribeiro, M. C. C. Vibrational Spectroscopy of Ionic Liquids. *Chem. Rev.* **2017**, *117*, 7053−7112.

(12) Izgorodina, E. I.; Seeger, Z. L.; Scarborough, D. L. A.; Tan, S. Y. S. Quantum Chemical Methods for the Prediction of Energetic, Physical, and Spectroscopic Properties of Ionic Liquids. *Chem. Rev.* **2017**, *117*, 6696−6754.

(13) Katsyuba, S. A.; Zvereva, E. E.; Vidis, A.; Dyson, P. J. Application of density functional theory and vibrational spectroscopy toward the rational design of ionic liquids. *J. Phys. Chem. A* **2007**, *111*, 352−370.

(14) Berg, R. W. Raman Spectroscopy and Ab-Initio Model Calculations on Ionic Liquids. *Monatsh. Chem.* **2007**, *138*, 1045−1075.

(15) Gatto, S.; Palumbo, O.; Caramazza, S.; Trequattrini, F.; Postorino, P.; Appetecchi, G. B.; Paolone, A. The infrared spectrum of bis(fluorosulfonyl)imide revisited: Attractive performances of the PBE0/6-31G** model. *Vib. Spectrosc.* **2016**, *82*, 16−21.

(16) Martinelli, A.; Matic, A.; Johansson, P.; Jacobsson, P.; Börjesson, L.; Fernicola, A.; Panero, S.; Scrosati, B.; Ohno, H. Conformational evolution of TFSI− in protic and aprotic ionic liquids. *J. Raman Spectrosc.* **2011**, *42*, 522−528.

(17) Mariani, A.; Bonomo, M.; Gao, X.; Centrella, B.; Nucara, A.; Buscaino, R.; Barge, A.; Barbero, N.; Gontrani, L.; Passerini, S. The unseen evidence of Reduced Ionicity: The elephant in (the) room temperature ionic liquids. *J. Mol. Liq.* **2021**, *324*, 115069.

(18) Köddermann, T.; Wertz, C.; Heintz, A.; Ludwig, R. The association of water in ionic liquids: a reliable measure of polarity. *Angew. Chem., Int. Ed.* **2006**, *45*, 3697−3702.

(19) Mori, K.; Kobayashi, T.; Sakakibara, K.; Ueda, K. Experimental and theoretical investigation of proton exchange reaction between protic ionic liquid diethylmethylammonium trifluoromethanesulfonate and H2O. *Chem. Phys. Lett.* **2012**, *552*, 58−63.

(20) Singh, D. K.; Rathke, B.; Kiefer, J.; Materny, A. Molecular Structure and Interactions in the Ionic Liquid 1-Ethyl-3-methylimidazolium Trifluoromethanesulfonate. *J. Phys. Chem. A* **2016**, *120*, 6274−6286.

(21) Danten, Y.; Cabaço, M. I.; Besnard, M. Interaction of water highly diluted in 1-alkyl-3-methyl imidazolium ionic liquids with the PF6(−) and BF4(−) anions. *J. Phys. Chem. A* **2009**, *113*, 2873−2889.

(22) Singh, D. K.; Donfack, P.; Rathke, B.; Kiefer, J.; Materny, A. Interplay of Different Moieties in the Binary System 1-Ethyl-3-methylimidazolium Trifluoromethanesulfonate/Water Studied by Raman Spectroscopy and Density Functional Theory Calculations. *J. Phys. Chem. B* **2019**, *123*, 4004−4016.

(23) Dong, K.; Song, Y.; Liu, X.; Cheng, W.; Yao, X.; Zhang, S. Understanding structures and hydrogen bonds of ionic liquids at the electronic level. *J. Phys. Chem. B* **2012**, *116*, 1007−1017.

(24) Tomasi, J.; Mennucci, B.; Cammi, R. Quantum mechanical continuum solvation models. *Chem. Rev.* **2005**, *105*, 2999−3094.

(25) Palumbo, O.; Cimini, A.; Trequattrini, F.; Brubach, J.-B.; Roy, P.; Paolone, A. The infrared spectra of protic ionic liquids: performances of different computational models to predict hydrogen bonds and conformer evolution. *Phys. Chem. Chem. Phys.* **2020**, *22*, 7497−7506.

(26) Giannozzi, P.; Baroni, S.; Bonini, N.; Calandra, M.; Car, R.; Cavazzoni, C.; Ceresoli, D.; Chiarotti, G. L.; Cococcioni, M.; Dabo, I.; et al. QUANTUM ESPRESSO: a modular and open-source software project for quantum simulations of materials. *J. Phys.: Condens. Matter* **2009**, *21*, 395502.
(27) Perdew, J. P.; Burke, K.; Ernzerhof, M. Generalized Gradient Approximation Made Simple. *Phys. Rev. Lett.* **1996**, *77*, 3865−3868.
(28) Vanderbilt, D. Soft self-consistent pseudopotentials in a generalized eigenvalue formalism. *Phys. Rev. B* **1990**, *41*, 7892−7895.
(29) Thompson, A. P.; Aktulga, H. M.; Berger, R.; Bolintineanu, D. S.; Brown, W. M.; Crozier, P. S.; in 't Veld, P. J.; Kohlmeyer, A.; Moore, S. G.; Nguyen, T. D.; et al. LAMMPS - a flexible simulation tool for particle-based materials modeling at the atomic, meso, and continuum scales. *Comput. Phys. Commun.* **2022**, *271*, 108171.
(30) Nasrabadi, A. T.; Gelb, L. D. Structural and Transport Properties of Tertiary Ammonium Triflate Ionic Liquids: A Molecular Dynamics Study. *J. Phys. Chem. B* **2017**, *121*, 1908−1921.
(31) Canongia Lopes, J. N.; Pádua, A. A. H. Molecular Force Field for Ionic Liquids Composed of Triflate or Bistriflylimide Anions. *J. Phys. Chem. B* **2004**, *108*, 16893−16898.
(32) Canongia Lopes, J. N.; Padua, A. A. H.; Shimizu, K. Molecular force field for ionic liquids IV: trialkylimidazolium and alkoxycarbonyl-imidazolium cations; alkylsulfonate and alkylsulfate anions. *J. Phys. Chem. B* **2008**, *112*, 5039−5046.
(33) Jorgensen, W. L.; Tirado-Rives, J. Potential energy functions for atomic-level simulations of water and organic and biomolecular systems. *Proc. Natl. Acad. Sci. U.S.A.* **2005**, *102*, 6665−6670.
(34) Dodda, L. S.; Vilseck, J. Z.; Tirado-Rives, J.; Jorgensen, W. L. 1.14*CM1A-LBCC: Localized Bond-Charge Corrected CM1A Charges for Condensed-Phase Simulations. *J. Phys. Chem. B* **2017**, *121*, 3864−3870.
(35) Dodda, L. S.; Cabeza de Vaca, I.; Tirado-Rives, J.; Jorgensen, W. L. LigParGen web server: an automatic OPLS-AA parameter generator for organic ligands. *Nucleic Acids Res.* **2017**, *45*, W331−W336.
(36) Atilhan, M.; Anaya, B.; Ullah, R.; Costa, L. T.; Aparicio, S. Double Salt Ionic Liquids Based on Ammonium Cations and Their Application for CO 2 Capture. *J. Phys. Chem. C* **2016**, *120*, 17829−17844.
(37) Miran, M. S.; Yasuda, T.; Susan, M. A. B. H.; Dokko, K.; Watanabe, M. Binary Protic Ionic Liquid Mixtures as a Proton Conductor: High Fuel Cell Reaction Activity and Facile Proton Transport. *J. Phys. Chem. C* **2014**, *118*, 27631−27639.
(38) Luo, H.; Yu, M.; Dai, S. Solvent Extraction of Sr2+ and Cs+ Based on Hydrophobic Protic Ionic Liquids. *Z. Naturforsch. A* **2007**, *62*, 281−291.
(39) Schrader, B.; Bougeard, D. *Infrared and Raman Spectroscopy: Methods and Applications*; VCH: Weinheim, Cambridge, 1995.
(40) Mori, K.; Hashimoto, S.; Yuzuri, T.; Sakakibara, K. Structural and Spectroscopic Characteristics of a Proton-Conductive Ionic Liquid Diethylmethylammonium Trifluoromethanesulfonate [dema][TfOH]. *Bull. Chem. Soc. Jpn.* **2010**, *83*, 328−334.
(41) Fumino, K.; Reichert, E.; Wittler, K.; Hempelmann, R.; Ludwig, R. Low-frequency vibrational modes of protic molten salts and ionic liquids: detecting and quantifying hydrogen bonds. *Angew. Chem., Int. Ed. Engl.* **2012**, *51*, 6236−6240.
(42) Fumino, K.; Stange, P.; Fossog, V.; Hempelmann, R.; Ludwig, R. Equilibrium of contact and solvent-separated ion pairs in mixtures of protic ionic liquids and molecular solvents controlled by polarity. *Angew. Chem., Int. Ed. Engl.* **2013**, *52*, 12439−12442.
(43) Ludwig, R. The effect of dispersion forces on the interaction energies and far infrared spectra of protic ionic liquids. *Phys. Chem. Chem. Phys.* **2015**, *17*, 13790−13793.
(44) Golub, B.; Fumino, K.; Stange, P.; Fossog, V.; Hempelmann, R.; Ondo, D.; Paschek, D.; Ludwig, R. Balance Between Contact and Solvent-Separated Ion Pairs in Mixtures of the Protic Ionic Liquid Et3NHMeSO3 with Water Controlled by Water Content and Temperature. *J. Phys. Chem. B* **2021**, *125*, 4476−4488.
(45) Fumino, K.; Bonsa, A.-M.; Golub, B.; Paschek, D.; Ludwig, R. Non-ideal mixing behaviour of hydrogen bonding in mixtures of protic ionic liquids. *Chemphyschem Eur. J. Chem. Phys. Phys. Chem.* **2015**, *16*, 299−304.
(46) Fumino, K.; Fossog, V.; Stange, P.; Paschek, D.; Hempelmann, R.; Ludwig, R. Controlling the subtle energy balance in protic ionic liquids: dispersion forces compete with hydrogen bonds. *Angew. Chem., Int. Ed. Engl.* **2015**, *54*, 2792−2795.
(47) Fumino, K.; Reimann, S.; Ludwig, R. Probing molecular interaction in ionic liquids by low frequency spectroscopy: Coulomb energy, hydrogen bonding and dispersion forces. *Phys. Chem. Chem. Phys.* **2014**, *16*, 21903−21929.
(48) Chen, Y. Spectroelectrochemical study of the oxygen reduction reaction at the interface between protic ionic liquids and a platinum electrode. Ph.D. Dissertation, RWTH Aachen University, 2024.

https://doi.org/10.1021/acs.jpcb.4c05084
J. Phys. Chem. B 2024, 128, 11723−11729